

ISOTOPE EFFECTS IN THE IONIZATION OF
GASES ON IMPACT OF METASTABLE
ATOMS

By
JAMES ROBERT FULTON

A DISSERTATION SUBMITTED TO THE FACULTY MEMBERS OF
THE GRADUATE SCHOOL
OF THE UNIVERSITY OF FLORIDA
IN PARTIAL FULFILLMENT OF THE REQUIREMENTS FOR THE
DEGREE OF DOCTOR OF PHILOSOPHY

UNIVERSITY OF FLORIDA

December, 1961

ACKNOWLEDGMENTS

The author would like to express sincere thanks to Dr. H. B. Hushkins, Jr., Chairman of his Supervisory Committee, for invaluable advice and assistance in the course of this research. He also wishes to thank the other members of his Supervisory Committee for their many helpful suggestions. To his fellow graduate students he expresses gratitude for their fellowship and for many discussions which served to ease a number of the frustrations which occur in such experimental work.

Finally, the author wishes to express gratitude to the National Science Foundation and to The Petroleum Research Foundation for the financial assistance which made this work possible.

TABLE OF CONTENTS

	Page
ABSTRACTS.....	ii
LIST OF TABLES.....	iv
LIST OF FIGURES.....	v
Chapter	
I. INTRODUCTION.....	1
II. HISTORY OF ISOLATION PROCEDURES INVOLVING RETAINABLE SPECIES.....	3
III. DESCRIPTION OF APPARATUS.....	12
IV. DESCRIPTION OF EXPERIMENTAL METHOD.....	14
V. EXPERIMENTAL PROCEDURES AND RESULTS.....	23
VI. DISCUSSION.....	41
VII. SUMMARY.....	52
BIBLIOGRAPHY.....	53
EXPLANATORY INDEX.....	57

LIST OF TABLES

Table	Page
1. Binding Energy With Which Forming Ions May Be Formed	49
2. Comparison of $\text{Be}^+ - \text{OH}_2$ and $\text{Be}^+ - \text{CH}_4$ Bond Spectra.	50
3. Comparison of $\text{Be}^+ - \text{OH}_2$ and $\text{Be}^+ - \text{CH}_4$ Bond Spectra with Previous Work	51

LIST OF FIGURES

Figure	Page
1. Schematic diagram of mass spectrometer	13
2. Schematic diagram of ion source.	14
3. Collision chamber pressure versus backing pressure	23
4. H_2^+ intensity versus H_2 backing pressure . . .	26
5. HD^+ intensity versus H_2 backing pressure . . .	27
6. H_2^+ intensity versus He backing pressure . . .	28
7. H_2^+ intensity versus F_2 backing pressure . . .	30
8. HD^+ intensity versus HD backing pressure. . . .	31
9. D_2^+ intensity versus D_2 backing pressure . . .	32
10. H_2^+ (charge transfer) and Ar^+ crossed curves .	34
11. H_2^+ and D_2^+ crossed curves	37
12. Ar^+ and H_2^+ crossed curves	38
13. H_2^+ crossed curve.	39
14. He^+ crossed curve.	40
15. Spectroscopic potential energy curves	45

CHAPTER I

INTRODUCTION

Atomic and molecular collisions may be categorized according to the status of the particles surviving the collision. If the particles are in status identical to those previous to the collision, then the event is said to be elastic. However, if the collision involves a transfer of either mass or internal energy it is termed inelastic.

Chemical reactions are a direct result of inelastic collisions, hence collisions of this type are of fundamental interest to the chemist. It is the interaction of molecular forces occurring during such an inelastic event which governs the outcome of a reaction. In the past, the majority of our information regarding intermolecular forces was obtained from bulk experiments. Subsequently, hypotheses were advanced to explain the microscopic phenomena which could successfully describe the microscopic phenomena observed. These hypotheses attempted to correlate viscosity, compressibility, acoustic pressure, phase changes and thermal properties with the nature of the microscopic events which could produce them. In order to

yield useful results, such experiments demanded far-sighted extrapolations and often complex theories. However, the recent development of scattering techniques has furnished a method to observe directly the microscopic processes in question. Scattering experiments enable the observer to investigate the lifetimes, concentrations and identities of reaction intermediates impossible to study otherwise.

One of the features of the new techniques involves the use of one or more scattered beams. Beams have been used extensively for the study of elastic as well as inelastic collisions.⁽¹⁾ The earliest reported beam experiments are those of Panzer⁽²⁾ who, in 1913, found that beams of sodium atoms allowed to effuse into a vacuum followed straight-line trajectories.

Significant improvements were introduced by Stern^(3,4) and subsequent workers. More recently, Gomer has reported the production of high velocity atomic and molecular beams⁽⁵⁾ and the use of such beams in the investigation of intermolecular forces.⁽⁶⁾ The first beam experiments involving a chemical reaction were those by Taylor and Eise⁽⁷⁾. The first reliable measurements of the elastic scattering cross sections for ions scattered by neutral molecules are due to Hammer and Eilstein⁽⁸⁾ in 1953. More precise determinations originated with Baselli, Fettes and Gomer⁽⁹⁾ in their study of total (elastic plus inelastic) scattering

cross sections for slow ions in gases. Later work by Simons and coworkers^(10,11,12,13,14) yielded separate cross sections for elastic and inelastic processes. Recently et al.,⁽¹⁵⁾ describe the determination of charge transfer cross sections for H^+ in the paper. In these collisions extractable hydrogen atoms are formed. The cross sections reported are about 40 \AA^2 for positive ion energies between 0.3 and 1 eV.

In 1938 Hays and Barham⁽¹⁶⁾ pointed out ion-molecule reactions such as



as possible sources of ions in mass spectrometry. The surprising appearance of secondary ions as formed was further reported by Bayth,⁽¹⁷⁾ Stevenson and Schindler⁽¹⁸⁾ and Field, Franklin and Loomis⁽¹⁹⁾ here, more recently, investigated these ion-molecular reactions and reported that they generally require little or no activation energy and proceed with extremely large rate constants. Glass and Hais⁽²⁰⁾ have extended the study of ion-molecule reactions to determine their dependence on the energy of the bombarding ion, and Michael⁽²¹⁾ has investigated reactions of the type



Extensive mass spectrometric studies of ionization phenomena resulting from electron impact have been conducted,

and numerous experiments using photon backscattering have been reported. However, another source of ionizing energy has only recently come under investigation. This source is the excitation energy of excited atoms and molecules, e.g.,

$$A^* + B \rightarrow A + B^* + e . \quad (1.3)$$

It is the aim of the work described here to investigate the effect of isotopic substitution in the molecule B upon the cross sections for such processes. A summary of our knowledge of collisions of this general type is given in the next chapter.

CHAPTER II

KINETICS OF DIELS-ALDER REACTIONS INVOLVING METASTABLE SPECIES

Excited states or isomers with lifetimes longer than one microsecond are usually considered metastable, with the transition to the ground state by the emission of electric dipole radiation being forbidden by one or more of the selection rules governing such decay. These rules are:

- (a) $\Delta l = 0, \pm 1$ $J = 0 \rightarrow J = 0$
- (b) $\Delta S = 0$
- (c) $\Delta l = \pm 1$

with

J = vector sum of L and S

L = orbital angular momentum

S = spin angular momentum

l = angular momentum of electron making the transition

Balzer has two metastable states which lie below the ionization potential, namely, the 2^3P_0 state at 22.61 ev. and the 2^3P_1 at 19.52 ev. above the ground state. Decay of the 2^3P_0 is forbidden by rules (a) and (c), and of the 2^3P_1 by (b) and (c). Neon possesses two metastable states, $3P_2$ and $3P_0$ at 16.62 ev. and 16.71 ev. while argon similarly has two, $3P_2$ and $3P_0$ with energies of 11.95 ev. and 11.72 ev., respectively.⁽²²⁾

These metastable helium species have lifetimes of the order of tenths of a second compared with the order of 10^{-8} seconds for most excited states with allowed decay transitions. Their loss may result from double photon emission and by magnetic dipole transitions; however, these processes are generally less than 10^{-5} times as frequent as electric dipole transitions.

Metastable atoms have been produced by electron bombardment, as used in this work, and from gaseous discharges. When electron bombardment is used, the excitation may take place just before the first beam defining slit, or with some loss of excitation just past the first or a later defining slit. When a gaseous discharge serves as the source of excitation energy, the discharge is said to take place in the high pressure region just before the first defining slit in the excitation system.

In the determination of cross sections involving these excited atoms, frequent use is made of the fact that if the beam of metastable particles is allowed to strike a metal surface whose work function is lower than the excitation energy of the incident particles the energy of excitation results in the ejection of electrons from the metal.⁽²⁸⁾ The resultant current to the metal surface may be measured with an electrometer to determine the beam flux. Lichten⁽²⁹⁾ has reported the use of an alkali metal surface to detect the $^3P_{2,0}$ states of mercury.

If one is to be made of the previously known excitation energies available in metastable atoms, it is necessary to be able to separate the affairs of excited states of differing energies when the excited species may exist at two or more metastable levels. Fikselott and Lichten⁽²⁵⁾ have described the use of circular beam magnetic resonance to separate the 3P_2 and 3P_0 metastable states of mercury, and have reported separate electron impact excitation functions for each state. More recently, Richards and Paschke⁽²⁶⁾ measured the ratio of 2^1S to 2^3S states by deflection of the excited beam in an inhomogeneous magnetic field. Series are reported for various energies of the exciting electron beam. These results were later refined, as reported by Bayle, Richards, and Paschke.⁽²⁷⁾ There is a pressure effect on the singlet to triplet ratio which arises partly from improvement of resonance radiation and partly from selective scattering of the two species.

When an excited species interacts with a target atom or molecule, several types of reactions may occur. General forms of these reactions are given below, where the excited species is the atom A^* and the target, the molecule X_0 .



All of the above processes leading to ionization require very little conversion of internal energy to kinetic energy of the product molecules since the electron can carry off as kinetic energy all the excitation energy of A^* above that necessary to initiate the reaction.

Reactions of types [II.3] and [II.6] are termed chemi-ionization or Bormbeck-Polmer reactions after their initial investigators.⁽²⁸⁾ Bormbeck and Polmer's work has more recently been extended by Field and Franklin,⁽²⁹⁾ and Patai and Itoh.⁽³⁰⁾ It is observed that chemi-ionization is most likely when the energy of the excited species A^* is near that required to initiate the reaction.⁽³¹⁾

Emmelfarb and Fiesing⁽³²⁾ made use of reactions of types [II.3] and [II.4] in explaining ionization of mixed rare gases in cold-cathode gaseous discharges. It is with reference to this early work that such reactions are termed Fiesing ionization. Jones and Redaelli⁽³³⁾ reported on the

role of Fanning ionization in the radio chemistry of gases. In 1962, Ferguson,⁽³⁴⁾ using a simple classical ionization-transfer collision model, showed that for a potential of the form $\propto \exp(-\delta r)$ the cross sections for Fanning ionization are given by

$$Q = 3\pi(12u/\pi g^2)^{1/3} A_1(\delta)$$

where

$$A_1(\delta) = 0.439, \text{ the collision integral calculated by Milne, Stegwee and Rice-Straussler}^{(35)}$$

u = reduced mass

g = relative velocity.

Smith and Macmillan⁽³⁶⁾ have investigated the elastic scattering of metastable helium beams in other rare gases, and more recently, Skolnik and Macmillan⁽³⁷⁾ measured cross sections for the Fanning ionization process with He^+ in H_2 and obtained separate cross sections for the singlet and triplet states of He^+ . Goussard and Goussard^(38,39) and Macmillan and Miles⁽⁴⁰⁾ have reported studies of Fanning ionization of hydrocarbons.

In 1958, Day, Rice-Straussler and Murphy⁽⁴¹⁾ obtained spectroscopic evidence of the existence of a heavy isotop of hydrogen in a sample of normal hydrogen which had been reduced to a small volume by distillation. The appearance of this isotop led to several theoretical

substitutions of the relative reaction rates of hydrogen and heavy hydrogen, termed isotopeism.

Cramer and Polanyi⁽⁴²⁾ predicted that hydrogens and deuteriums should react at different rates as a result of their differing zero-point energies.⁽⁴³⁾ Spring and Shomon⁽⁴⁴⁾ also predicted this theoretical difference in reaction rates. Pines and Wigner⁽⁴⁵⁾ and Eyring, Spring and Taylor⁽⁴⁶⁾ are responsible for early application of "absolute rate" theory to the two isotopes of hydrogen, along with Wigner, Taylor and Spring.⁽⁴⁷⁾ Bigeleisen⁽⁴⁸⁾ has applied the theory to rate constants involving isotopically substituted molecules. The predicted rate for the light molecule is greater than that for the heavy molecule by the square root of the inverse ratio of the reduced masses. A brief adaptation for the case of molecular decomposition of I_2^* follows.

From "absolute rate" theory the rate of a reaction in which I_2^* dissociates to give 2I may be written:

$$k = K \cdot Q^* \left(\frac{kT}{2\pi\mu^*} \right)^{1/2} \frac{1}{\bar{h}} \quad \text{(III.7)}$$

where K is the transmission coefficient, Q^* is the concentration of the excited molecule and μ^* the effective mass along the coordinate of decomposition and \bar{h} is the length of the top of the potential barrier which the excited molecule traverses. For isotopes of I_2^* with effective masses

a_1^* and a_2^* and with dissociation rates k_1 and k_2 a set of rate constants may be written from (II.7) as before, assuming β to be equal for the isotopic molecules,

$$\frac{k_1}{k_2} = \frac{\Sigma a_1^*}{\Sigma a_2^*} \left(\frac{a_2^*}{a_1^*} \right)^{1/2} . \quad (\text{II.8})$$

In the experiments to be described here it must be assumed that $a_1^* = a_2^*$ and that the transmission coefficients Σ_1 and Σ_2 are also equal. Then (II.8) simplifies to

$$\frac{k_1}{k_2} = \left(\frac{a_2^*}{a_1^*} \right)^{1/2}$$

or

$$k_1 a_1^{1/2} = k_2 a_2^{1/2} . \quad (\text{II.9})$$

Since, k_2 may be replaced by the quotient of a zero independent rate constant k_2^* and a_2^* as

$$k_2 = \frac{k_2^*}{a_2^*} , \quad (\text{II.10})$$

The prediction of isotopic effects for Pillingham reaction advanced by Fickman and Jones^(49,50) is considered in this work. The first observation of the isotopic effect is due to Jones.⁽⁵¹⁾

CHAPTER III

DESCRIPTION OF APPARATUS

The experimental arrangement used for this work consists of a 180° radius-of-curvature, 60° sector, magnetic deflection, first order direction-focusing mass spectrometer with a theoretical resolution of 1:2000. The spectrometer is schematically represented in Figure 1. It is essentially the same instrument as used by Wiley⁽¹²⁾ in his work.

The ion source which occupies regions 1 and 2 in Figure 1 is illustrated in Figure 2. The region 2 consists of a conventional thermionic emission, electron bombardment source which may be used to produce either ions or excited species, according to the experiment being conducted. The electron gun employs an iridium ribbon filament F cathodically coated with thorium oxide according to MacKilts, Randolph and Bebb.⁽¹³⁾ The product beam from the source passes between the deflecting and focusing electrodes E_1 (12), through the focusing electrode E_2 , and into the collision chamber C defined by electrodes E_2 and A_1 and insulated from E_2 by a ceramic slug L . The ion source has been modified by the addition of a metal ring T

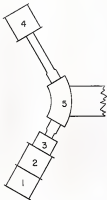


Fig. 1.-Schematic diagram of mass spectrometer.

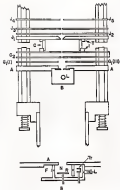


Fig. 2.—Schematic diagram of ion source.

collected to the top of the collision chamber and having the legs contacting I_1 bugged to insure close fit. The increased gas leakage path permits collision chamber pressures greater than 10^{-5} torr without flooding other portions of the spectrometer. The electron gun assembly has been cleaned and realigned, and a new filament installed. The new filament is of smaller cross section and its operating current is found to be more compatible with the power capabilities of the emission regulator circuit used for control. These modifications result in an increase of approximately one hundred-fold in secondary beam intensity over that reported by Weiss.⁽³⁴⁾

By proper selection of potentials applied to the repeller electrode R , and the electrodes E_1 and E_2 , ions from the source region S may be either focused into the collision chamber or, they may be deflected away allowing any neutral ground state or excited particles to proceed into the collision chamber unaffected. Ions produced in the collision chamber may be extracted into the analyzer by application of an appropriate potential between E_2 and E_1 to establish a directed field between these electrodes. The beam gas is leaked into the source at L through a Tucksonic "Ford-Tec" leak valve. The scattering gas is introduced into O through a similar Tucksonic valve. Separate gas handling systems are provided to enable the

introduction of different gases into the source and collision regions without the necessity of using gas mixtures. The mass spectrometer, and collision chamber and ion source components are fabricated from Inconel with the exception of minor parts of nickel, tungsten, stainless steel and gold. The focusing electrodes are cut from 0.02% inch Inconel sheet. The electrode stack is supported on and held in alignment by four precision ground glass rods of 0.020 inch diameter. The individual electrodes are separated by sleeve spacers cut from glass tubing of inside diameter slightly greater than the support rods. Only two of these rods are shown in Figure 1.

Ions emanating from the slit in the E_1 face of the collision chamber are gradually accelerated through a potential difference of five kilovolts obtained from a Furukawa Scientific Company high voltage power supply, model 10000. In the course of this acceleration, the ion beam is focused by a series of electrostatic lenses contained in region 3 (Fig. 1). The ion beam is then analyzed by a homogeneous magnetic field in region 5. The deflected beam traverses the field-free flight tube to region 6 where it passes through an adjustable slit and strikes the detector which may be chosen to be a simple metal plate or the first dynode of an electron multiplier according to the distance of the ion beam intensity. The

multipplier is a 18 stage device having copper-beryllium dynodes. It was manufactured by Radio Electronics Associates as their model EM-1. The high voltage for the multiplier is obtained from a Northeast Scientific Company model 5000 power supply. During the course of this work the gain of the multiplier was observed to remain constant at slightly less than 10^5 for 10^7 ions. The field current of the analyzer magnet is controlled by an electronically regulated and swept power supply constructed in these laboratories. The magnet coils are of high impedances, low current design. The magnetic field is determined within 0.01 per cent by a Harvey Wells 500 Gaussmeter. The output current of either the single collector or the electron multiplier is passed through a high resistance ($10^8 - 10^{10}$ ohms) and the voltage thus developed measured by a Cary vibrating reed electrometer and recorded by a 6 inch Ebert Associates chart recorder.

The helium, neon, argon, hydrogen, deuterium and nitrogen were obtained from cylinders and were purified by passage through an absorption trap filled with degassed charcoal at low temperature. These gases are estimated to have less than one part in 10^5 impurities as indicated by mass analysis. The methane used was Phillips Company reagent grade and guaranteed not to contain more than forty parts impurity per 10^5 . The methane- d_4 and D_2 were taken

from glass flasks sealed directly into the auxiliary vacuum manifold. The acetone-d₆, a Eichen Incorporated product, was observed to contain approximately one part impurity per 10³, and the K2 supplied by Eichen, also, had less than five parts per 10⁵ contamination, which consisted primarily of K₂ and D₂.

CHAPTER II

DESCRIPTION OF EXPERIMENTAL METHOD

The study of ionization processes described here involves the generation of a beam of rare gas atoms which contains atoms in metastable excited states. An excited beam is allowed to traverse a scattering volume, filled with a target gas, inside which a small portion of the incident beam is inelastically scattered. The ions produced by these resonant collisions are extracted from the collision chamber by the application of an appropriate electrostatic field within the chamber and are then subjected to analysis by a mass spectrometer.

At sufficiently low scattering gas pressures, Beer's law for absorption is applicable. That is,

$$dI_s/dz = I_p I_s \mu \quad (II.1)$$

where

I_p = primary beam intensity

I_s = secondary ion intensity

$\mu = 5.54 \times 10^{28}$ = the number of collisions per cm^3 at 1 torr pressure and 0 degree C

z = scattering path length

p = pressure is here corrected to 0°C
 σ = absorption cross section for
 reaction in cm².

Manipulation of (17.1) yields the more useful expression

$$I_p/I_p = I_p l p \sigma \quad (17.2)$$

If the scattering path length, l , and the pressure over l , p , are known the cross section may be calculated from the measured ratio I_p/I_p .

With the current apparatus, however, it is not possible to measure the primary beam intensity I_p . However, the primary beam intensity can be maintained constant, and hence ratios of cross sections for different scattering gases may be obtained. From (17.2) this ratio may be expressed

$$\sigma_1/\sigma_2 = I_{p1} p_2 / I_{p2} p_1 \quad (17.3)$$

With constant I_p and l a plot of I_p versus p gives a straight line with slope $I_p p_0 l \sigma$. Hence, the ratio of two absorption cross sections is given by the ratio of the two slopes

$$\frac{\sigma_1}{\sigma_2} = \frac{dI_{p1}/dp_1}{dI_{p2}/dp_2} \quad (17.4)$$

Using these ratios for an isotopic series such as I_2 , SO_2 , S_2 , it is necessary only to know the true cross section for one member of the series to determine that for each member.

CHAPTER V

EXPERIMENTAL PROCEDURE AND RESULTS

In all experiments the mass spectrometer was focused to optimum response for the ions expected to be observed, that is, when H_2 was the target gas, the focusing was optimized for H_2^+ ; when D_2 was the target gas the instrument was peaked for D_2^+ .

In order to determine pressures in the collision chamber for the H_2 , D_2 , and HD experiments, use was made of the H_2 , H_2^+ and D_2 , D_2^+ charge transfer cross sections reported by Green and Haxton.^(34,35) The charge transfer cross section for 50 volt H_2^+ ions in H_2 was taken as 8.2 \AA^2 and for 50 volt D_2^+ ions in D_2 as 9.5 \AA^2 . The cross section for 50 volt HD^+ ions in HD was taken to be the mean of these two, or 8.5 \AA^2 .

The procedure, as used by Kerdowsky,⁽³⁴⁾ for the pressure determinations is described below for hydrogen, but is identical for the isotopic gases similarly introduced into the instrument.

Hydrogen was leaked into both the source and collision chambers. The H_2^+ ions were generated in the source and focused into the collision chamber by adjustment of the

potentials on the deflection electrodes ϕ_1 (I) and ϕ_1 (II) (Fig. 2). The ion current to J_1 could then be measured as a function of pressure in the reservoir in back of the leak valves through which hydrogen was admitted to the collision chamber. By measuring the J_1 current at two potentials between J_1 and ϕ_2 it was possible to obtain values for both the primary ion current and the charge transfer, or secondary, ion current.

To determine these currents, ϕ_1 , ϕ_2 and J_1 were set at -60 volts with respect to F and J_2 made approximately 70 volts positive with respect to J_1 (by use of an external battery connected between J_1 and J_2). The grids was set at about 40 volts with respect to the filament. The current to J_1 was then measured with J_2 minus and plus four volts with respect to ϕ_2 . The former value was taken as the primary ion current and the latter as the primary ion current less the secondary ion current. Hence, the difference of the two values is the secondary ion current. A Hewlett-Packard DC Micro Voltmeter, Model 4234B, was employed in these measurements.

From the data collected as described above pressures were calculated and plotted against the backing pressure in a 12 liter reservoir behind the leak valves. This backing pressure was measured with a mercury manometer. The results are shown in Figure 3. The slope of the E_2 curve is

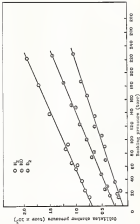


Fig. 3. Bubble point pressure versus bubble pressure.

5.60×10^{-6} and that for H_2 , 4.18×10^{-6} . In each case the pressures observed were in the 10^{-3} torr range. The failure of the curves to extrapolate through zero was attributed to diffusion of gas from the ion source into the collision chamber where it would be observed as a background pressure.

The procedure used for the production of metastable atoms is described below. The rare gas to be excited was introduced into the source and the ion beam thus produced was focused through the collision chamber as outlined above and through the spectrometer in standard fashion. Then the repeller electrode B was set at the filament potential and the deflection electrodes $G_1(I)$ and $G_2(II)$ were adjusted to their maximum deflection potential of 40 volts. The electrode, G_1 , was made five volts negative with respect to the anode (still at 40 volts). This negative potential on G_1 was found necessary to minimize electron leakage into the collision chamber. With the electrode potentials set in this manner, the complete elimination of ions entering the collision chamber was confirmed by the fact that no ions of the rare gas could be detected in the mass spectrum. The metastable atoms, however, are unaffected by the electric fields and diffuse through the electrode slits into the collision chamber. Under these conditions any ions observed in the mass spectrum must have been produced by Penning ionization in the collision chamber.

For all experiments on the relative cross sections for Penning ionization of isotopic hydrogen the D_2 - D_2 discharge potential was set at 35 volts as found by Karsenty⁽¹⁹⁶⁵⁾ to be optimum for the extraction of the various isotopic hydrogen ions.

In the He^+ , D_2 ($D_2 = D_2$, HD, D_2) systems only the D_2^+ ion was observed. No indication was found of the formation of H^+ , D_2^+ , HD^+ , etc., despite the fact that the metastable helium atoms have sufficient energy for dissociative ionization.

Plots were made of ion current against helium backing pressure for D_2^+ (Figure 4), He^+ (Figure 5) and D_2^+ (Figure 6). In each case the curve was found to be linear and to extrapolate through zero. The linear behavior described supports the thesis that, since the He^+ ion intensity is a linear function of helium backing pressure, the ionization must occur in single collisions of excited helium atoms with D_2 , HD or D_2 molecules. This thesis is further supported by the fact that the Penning ions appear at an electron energy of about twenty volts, thus eliminating the possibility of ion-molecule reactions with He^+ ions whose formation requires an electron energy of 24.38 volts.

In order to determine the relative Penning ionization cross sections for D_2 , HD and D_2 the positive ion

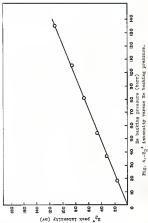


Fig. 4. P_g^0 intensity versus the backing pressure.

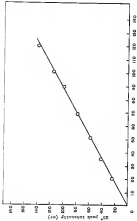


Fig. 3.— 10^4 intensity versus 10^4 loading pressure.

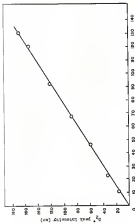


Fig. 4. $\log R_p$ versus $\log [M]$ for the polymerization of styrene.

current was plotted against collision chamber backing pressure for each of the three gases (Figures 7, 8, 9). The slope for N_2^+ versus N_2 was found to be 2.60, that for H_2 to be 2.46 and that for O_2 to be 2.54. According to equation (11.4) this gives ratios of absorption cross sections $\sigma_{\text{N}_2}/\sigma_{\text{N}_2}$ equal to 0.587 and $\sigma_{\text{H}_2}/\sigma_{\text{N}_2}$ equal to 0.794. These ratios must be corrected for the differences in the slopes of the pressure calibration curves; a factor of $3.60/4.18$ for O_2/N_2 and $3.60/4.40$ for H_2/N_2 . Also a correction for the variation of the electron multiplier gain with different ions must be considered. This represents a factor for $4.3 \pm 10^3/4.6 \pm 10^3$ for O_2/N_2 and of $4.3 \pm 10^3/4.75 \pm 10^3$ for H_2/N_2 . The corrected values for the ratios of the absorption cross sections are

$$\frac{\sigma_{\text{O}_2}}{\sigma_{\text{N}_2}} = 1.15 \quad (7.1)$$

$$\frac{\sigma_{\text{H}_2}}{\sigma_{\text{N}_2}} = 1.12 \quad (7.2)$$

The above ratios are those obtained directly from the experimental data and involve absorption cross sections obtained for a target gas with Maxwellian velocity distribution being traversed by a beam whose particles have a slightly modified Maxwellian distribution. The observed absorption cross section is dependent upon the relative

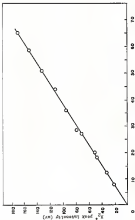


Fig. 3. $(\Delta T_b)^2$ tabulated versus P_b boiling pressure.

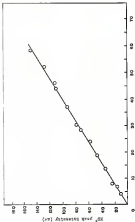


Fig. 5. 10^4 peak intensity versus 10^3 backing pressure.

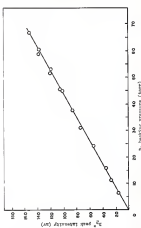


Fig. 2. $\sqrt{\sigma_1 - \sigma_2}$ tensile stress versus P_2 testing pressure.

velocity of the colliding species and is not a true cross section. The true cross section, Q_1 , is defined for the case of an incident particle of known velocity striking a target particle at rest. In order to obtain true cross sections, Q_1 , from experimentally determined absorption cross sections, σ_1 , it is necessary to apply corrections to the σ_1 . These corrections serve to relate the experimental data to an idealized system in which the incident beam is of homogeneous velocity and the particles of the target gas are at rest.

The correction described by Smith and Egan⁽³⁷⁾ makes no provision for various scattering potentials but presumes hard-sphere interactions. This is generally a very poor approximation to the true nature of a molecular collision interaction. In thermal energy collisions it would not be likely that anything approaching a hard-sphere interaction would be realized. Rather, a much softer interaction would be expected with a potential of the form $-e/r^n$ with n in range of 6 to 12. Beckling et al.,⁽³⁸⁾ have calculated correction factors with provisions for different potentials and have tabulated values for $e=6$ and $e=12$. The results, using the method of Beckling et al., with $e=6$, are, from [V.1] and [V.2]

$$\bar{Q}_{H_2}/\bar{Q}_{H_2} = 1.26 \quad (7.3)$$

$$\bar{Q}_{H_2}/\bar{Q}_{H_2} = 1.10 \quad (7.4)$$

Both the pressure calibration and Penning ionization measurements were repeated for hydrogen and deuterium. The results obtained were, within experimental error, the same as those reported here. These results differ from the preliminary measurements obtained by Erdosch.⁽¹⁴⁾ The only explanation that can be offered is that a gaseous discharge can occur within the accelerating structure when high pressures are used in the source or collision chamber. The pressures used by Erdosch were not sufficiently low to eliminate the possibility of such a discharge.

Of the measurements involved in the determination of these ratios those of pressure measurement in the collision chamber and ion current for the Penning process are believed to establish the limits of reliability of the data. A figure of reliability can only be approximated. The ratios of cross sections are estimated to be accurate to approximately ± 10 per cent.

It was noted by Erdosch⁽¹⁴⁾ that the Penning produced H_2^+ ions possessed considerable kinetic energy. Further investigations of this kinetic energy and its dependence upon the nature of the species being ionized were conducted in a manner described below.

With the source set up to study Feeding limitation, as previously described, the extraction potential applied between β_2 and β_1 was varied from zero through a maximum of about 50 volts. This extraction voltage was measured with a Sensitive Research Instruments Corporation Model JTW voltmeter. The areas under the ion current peaks were plotted against the imposed voltage and the curves for various systems are shown in Figures 10, 11, 12, 13, 14. The peak areas were determined by counting squares on the recorder chart and by weighing cutouts of the peaks. It was found that a plot using peak height instead of area yielded a severely distorted imposed potential curve. This distortion was attributed to the increase in energy spread of the ions, and hence, in peak width as the imposed potential was made larger.

Further investigation of the leakage effect in Feeding limitation was conducted with the systems Na^+ in CH_4 and CD_4 . A tabulation of the mass spectrum is presented in Table 2. A comparison of the Na^+ - CH_4 results with previous work by Čerešák and Herman⁽³⁰⁾ and Hunsballe and Vines⁽⁴²⁾ is given in Table 3.

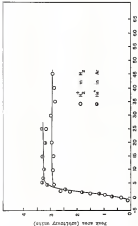


Fig. 10. H_2^+ (change transition) and H_2^- (change transition).

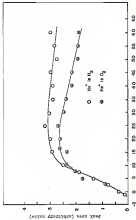


Fig. 11. H_2 and D_2 reversed curves.

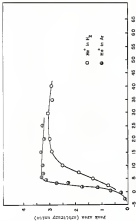


Fig. 12.— H_2 and Ar desorption curves.

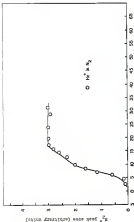


Fig. 11. H_2^+ streamer spectra.

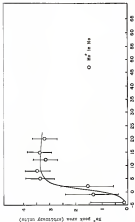


Fig. 14-8d. R_p vs. $[I]$ (mole/l.)

CHAPTER VI

DISCUSSION

It is apparent from the results described in the previous chapter that any proposed mechanism for the Penning ionization process must explain two characteristics to be successful. The first of these to be considered is the appearance of kinetic energy in the Penning ion, the second is the isotope effect observed in Penning ionization of isotopic hydrogen.

The kinetic energy with which the Penning ion is formed must come from conversion of some of the energy of the metastable atom in excess of that required to produce the ion. This conversion implies the formation of an intermediate complex which may then dissociate to yield a ground state rare gas atom and a target molecule in an excited ionizing state. This sequence is illustrated below,



Alternatively, the excited complex may alternatively lose an excited ion which further dissociates as shown in [VI.2].



either [VI.1] or [VI.2] can explain the formation of a feeding ion with kinetic energy though one would expect that the escaping electron in [VI.2] would carry away a large portion of the excess energy of excitation. However, assuming the concentration of the initial complex $(\text{Al}_2)^+$ is independent of the isotopic substitution of X_{20} , reaction [VI.2] offers an explanation of the isotope effect since the loss of an electron from the complex should be independent of the masses of the nuclei.

Now, reaction [VI.1] will be examined. If competing paths for destruction of X_2^+ are postulated as in [VI.3] the isotope effect may be rationalized.



This mechanism was first postulated by Flatau⁽⁴⁹⁾ in order to explain the results obtained by Jena.⁽⁵¹⁾ These results indicated an isotope effect in the ionization of contaminated rare gases when isotopic substitutions were made in the contaminants. Again it is expected that k_1 should be independent of the isotope since the probability of loss of the electron should not depend on the mass of the nucleus. But the dissociative reaction, unlike the ionization, involves relative nuclear motion and hence, the corresponding

rate constant k_2 would be expected to depend upon the molecular masses. From the results of absolute reaction rate theory given in Chapter II, it may be shown that

$$k_2 = k_2' (u)^{3/2} \quad (\text{II.10})$$

where k_2' is independent of mass and u is the reduced mass of the isotopic molecule. Thus p , the probability of ionization of I_2^* , may be written as

$$p = \frac{k_1}{k_1 + k_2'} = \frac{k_1}{k_1 + k_2' / (u)^{3/2}} \quad (\text{II.11})$$

If the ionization cross section Q_i is taken to be proportional to the probability of ionization p for a molecule of reduced mass u , a ratio of Q_i 's for two isotopes with reduced masses u_1 and u_2 may be written as

$$\frac{Q_{i1}}{Q_{i2}} = \frac{k_1 + k_2' / (u_2)^{3/2}}{k_1 + k_2' / (u_1)^{3/2}} \quad (\text{II.12})$$

The above mechanism is adopted from that proposed by Plattman,⁽⁴⁹⁾

From the ratios determined in these experiments the ratio k_1/k_2' may be evaluated. Using ratios of cross sections corrected according to Bickling $\underline{Q_{i1}/Q_{i2}}$, with $u = 0$ the ratio k_1/k_2' obtained for Q_{i1}/Q_{i2} is

$$\frac{k_1}{k_2} = 0.63 \quad (11.6)$$

and for Q_{22}/Q_{12}

$$\frac{k_1}{k_2} = 0.53 \quad (11.7)$$

This agreement can be considered very good in view of the fact that the computations involve relatively small differences in large numbers. If $\epsilon = \infty$ is used, completely inconsistent results are obtained. It should be noted that above considerations produce no isotope effect in the formation of the intermediate complex.

The transfer of energy from the metastable atom to the target molecule through the perturbed complex may be described in terms of potential energy curves as shown in Figure 1j. If the potential energy curves of $A^* + B$ and $A + B^*$ occur as in Figure 1ja there is a probability that $A^* + B$ entering along its curve will, if the A^*B separation drops below the intersection point r_c , separate along the potential energy curve for $A + B^*$, converting a fraction of the excitation energy of A^* into kinetic energy, represented by the separation of the horizontal portions of the two curves, and transferring the remainder into excitation of B . It is conceivable that the $A^* + B$ curve is repulsive, Figure 1jb, in which case the curves would not be



15a



15b

Fig. 15.-Hypothetical potential energy curves.

likely to occur except at very small separations which are not likely to be realized in thermal energy collisions. This might explain the fact that no Penning ionization was observed in the system $\text{He}^+ + \text{I}_2$ even though the metastable neon atom has sufficient energy to ionize hydrogen. A discussion of these potential energy curve intersections may be found in Herzberg.⁽⁴⁴⁾

All species investigated in these experiments have been found to have several subionizing levels within a volt of their ionization threshold. Dubster, Kiese and Krone⁽⁵³⁾ have reported such levels in H_2 , H , D_2 and D ; Halfen, Tanaka and Larabee^(54,55) have seen them in H_2 . The ion will appear with maximum kinetic energy if it is formed from a molecule in the lowest subionizing state. Table I shows the excess energy available from the rare gas metastable atom, and the maximum amount of kinetic energy with which the ion may appear, assuming that the lowest subionizing state is involved and that the energy of this state is negligibly above the lowest ionization potential. This maximum kinetic energy is calculated from simple mass considerations to be

$$E_{\text{max}} = \frac{M_A}{M_A + M_{X_2}} (E_A - E_I) \quad (\text{VI-6})$$

where

E_{max} = the maximum kinetic energy which may appear in the ion

m_A = mass of the aristobles atom

m_{X_2} = mass of X_2

E_A = excitation energy of aristobles atom

E_i = ionization potential of X_2

In the slowest potential curves (Figs. 10a14) it is seen that as the mass of the ion increases, kinetic energy decreases, approaching thermal energy for Ar^+ . This is evident from the fact that smaller slowest potentials are required to completely extract the heavier ions. The standard curve for essentially thermal energy ions is that for charge transfer of X_2^+ in X_2 . This process has been shown to produce ions with very little kinetic energy by Slone et al.,⁽¹³⁾ and Gross and Slone.⁽¹⁴⁾ Charge transfer curves for X_2^+ in X_2 obtained here (Fig. 10) agree well with those of the former authors whose apparatus had a similar geometry to that used here.

Further investigation of isotope effects was conducted in the systems Se^+ and Te^+ in CH_4 and CD_4 . Absolute cross sections could not be considered in these systems since the lack of appropriate charge transfer cross sections made it impossible to determine collision number processes. A comparison of spectra obtained with Se^+ in CH_4 and CD_4 is given in Table 3. The experiment was

performed using different energies for the electrons exciting the helium atoms. These results are listed with the ratio of singlet to triplet metastable atoms found by Bogan.⁽¹²⁷⁾ The singlet to triplet ratio increases as the energy of the electrons used in excitation is increased. It may thus be concluded that the increase in relative abundance of CH_2^2 with increase in electron energy is an isotope effect due primarily to the singlet state of the metastable helium.

Table I compares the results of this work with those of Bernick and Barrow⁽¹²⁸⁾ and Washburn and Weiss⁽¹⁴⁰⁾ for ionizing calibration of metastable neon and helium in CH_4 . Argon was also used, but in no case was any ionization observed. The agreement using the He^+ data is good, and that with He^+ not metastable when consideration is given to the low intensities of product ions in this case. The data reported here is considerably more precise than that of Washburn and Weiss, since greater ion currents were obtained by the previously described modifications in the apparatus.

TABLE 1
MAXIMUM ENERGY WITH WHICH PHOTONS CAN BE FORMED

$$E_{\text{max}} = \frac{E_A}{n_A + n_{X_0}} \quad (E_A = E_1)$$

Retardable Atom and Energy	Target Atom and Ioniza- tion Energy	n_A	E_{max}
Hg ⁺ (20.6 ev.)	H ₂ (13.4 ev.)	5.2 ev.	3.9 ev.
(20.6 ev.)	He (25.4 ev.)	5.2 ev.	3.9 ev.
(20.6 ev.)	Ne (23.4 ev.)	5.2 ev.	3.6 ev.
(20.6 ev.)	Ar (15.6 ev.)	3.9 ev.	3.63 ev.
(20.6 ev.)	Ar (15.8 ev.)	4.8 ev.	3.44 ev.
Hg ⁺ (28.7 ev.)	H ₂ (13.6 ev.)	5.1 ev.	3.46 ev.

TABLE 2
COMPARISON OF $\text{Fe}^{2+} - \text{CO}_2$ AND $\text{Fe}^{3+} - \text{CO}_2$ FLUO SPECTRA

Fluorescence quantum yield = 30 %, $\lambda^{\text{exc}} / \lambda^{\text{em}} = 2.6$				
Time	n = 4	n = 3	n = 2	n = 1
CO_2	49.2	52.1	54.7	-
CO_2	49.0	53.7	54.3	-
Fluorescence quantum yield = 40 %, $\lambda^{\text{exc}} / \lambda^{\text{em}} = 1.8$				
CO_2	49.7	53.8	54.3	-
CO_2	48.7	53.6	54.7	-
Fluorescence quantum yield = 50 %, $\lambda^{\text{exc}} / \lambda^{\text{em}} = 1.5$				
CO_2	53.8	54.0	54.8	-
CO_2	53.7	54.6	54.3	54.4

TABLE 3
COMPARISON OF $\text{Fe}^{2+} + \text{CH}_4$ AND $\text{Fe}^{2+} + \text{CH}_3$ REACTION RATES
WITH PREVIOUS WORK

Investigator	Barnhill, Korman (1955)		Barnhill & Wolke (1961)		Fenton & Barnhill (1966)	
	Fe^{2+}	Fe^{2+}	Fe^{2+}	Fe^{2+}	Fe^{2+}	Fe^{2+}
CH_4^a	43.5	38.1	32.4	32.5	-	40.7
CH_3^b	52.8	56.2	45.0	51.9	-	58.6
CH_2^c	3.3	3.7	2.6	10.2	-	3.3
CH^d	0	0	0	0	-	0

CHAPTER VII

SUMMARY

A high-resolution mass spectrometer was used to investigate inelastic collisions of metastable helium atoms in H_2 , HD , D_2 , Ar , Ne and Cl_2 . The metastable atoms were produced in an electron bombardment source and collimated into a beam. The beam was allowed to traverse a gas-filled collision chamber. Ions formed in the collision chamber were extracted and analyzed in the mass spectrometer. Processes in the collision chamber were determined from measurements of the appropriate systematic charge transfer for H_2 , HD and D_2 , and from the known cross sections for this process.

An isotopic effect is noted in the ionization of H_2 , HD and D_2 with the H_2^+ cross section 1.35 times that of H_2^+ and the HD^+ cross section 1.15 times that for H_2 . The ions are observed to have appreciable kinetic energy. A mechanism is proposed to explain the isotopic effect and the appearance of kinetic energy in the product ions.

Further investigations were conducted with metastable helium in methane and methane- d_4 .

BIBLIOGRAPHY

1. R. F. Snider, "Molecular Beams," Oxford University Press, London (1956).
2. R. Snider, *Compton Rend.* 55, 394 (1951).
3. G. Stern, *Zeits. f. Physik* 33, 750 (1934).
4. G. Stern, *Zeits. f. Physik* 41, 563 (1937).
5. I. Adler and A. L. Reinegar, *J. Chem. Phys.* 22, 664 (1954).
6. I. Adler, E. A. Hagen, and J. E. Jordan, *J. Chem. Phys.* 22, 307 (1953).
7. L. B. Feller and S. Deha, *J. Chem. Phys.* 23, 1711 (1954).
8. G. Humberston and E. Kellath, *Ann. Geo Physik* 13, 300 (1933).
9. L. H. Russell, G. E. Fickens, and J. E. Sloness, *J. Chem. Phys.* 3, 365 (1945).
10. J. E. Sloness, E. T. Francis, G. E. Fickens, and S. E. Jackson, *Rev. Sci. Instr.* 13, 413 (1942).
11. J. E. Sloness, G. E. Fickens, E. E. Henschelitz, Jr., and S. E. Jackson, *J. Chem. Phys.* 11, 307 (1943).
12. J. E. Sloness, G. E. Fickens, E. T. Francis, and L. G. Eager, *J. Chem. Phys.* 11, 313 (1943).
13. J. E. Sloness, E. T. Francis, E. E. Henschelitz, Jr., and S. G. Papenag, *J. Chem. Phys.* 11, 314 (1943).
14. J. E. Sloness, E. E. Henschelitz, Jr., and L. G. Eager, *J. Chem. Phys.* 11, 308 (1943).
15. E. L. Boudally, E. Clapp, W. Sawyer, and H. Schultz, *Phys. Rev. Letters* 12, 303 (1954).

16. T. E. Eyring and E. M. Eyring, *Phys. Rev.* **12**, 786 (1938).
17. E. E. Gajda, *Rev. Mod. Phys.* **1**, 347 (1931).
18. J. F. Starnes and E. G. Schlesier, *J. Chem. Phys.* **22**, 1255 (1955).
19. J. E. Field, J. L. Franklin, and F. W. Lampe, *J. Am. Chem. Soc.* **79**, 3413 (1957).
20. G. F. Giese and W. E. Miller, *J. Chem. Phys.* **32**, 1465 (1961).
21. E. Lindholm, *Arkiv. Fysik* **2**, 257, 453 (1954).
22. E. E. Hershler, Jr., Chapter of "Advances in Chemical and Physical," Ed. by John Deane, John Wiley and Sons, New York (to be published).
23. E. Mercuriano, *Papier* **2**, 443, 447 (1962).
24. W. Claitor, *Phys. Rev.* **102**, 1231 (1956).
25. H. A. Mahan and W. L. Smith, *Phys. Rev.* **123**, 134 (1961).
26. E. L. Richards and E. E. Hershler, Jr., *J. Chem. Phys.* **31**, 557 (1959).
27. J. L. G. Pagan, E. L. Richards, and E. E. Hershler, Jr., *Brit. Am. Phys. Soc.* **12**, (2) 161 (1965).
28. J. Noyes and J. F. Holnar, *Phys. Rev.* **121**, 621 (1961).
29. F. E. Field and J. L. Franklin, *J. Am. Chem. Soc.* **83**, 4307 (1961).
30. R. Fuchs and W. Kuhl, *Z. Naturforschung* **15a**, 328 (1960).
31. H. E. B. Farnum, F. E. Field, and J. L. Franklin, *J. Chem. Phys.* **32**, 1770 (1960).
32. A. A. Krotzoff and F. W. Zwending, *Papier* **1**, 430 (1967).
33. W. F. Jones and J. Rudnicki, *Phys. Rev.* **102**, 1755 (1956).

34. E. E. Ferguson, *Phys. Rev.* 122, 822 (1962).
35. E. J. Hinson, D. E. Stogryn, and J. O. Hirschfelder, *Phys. Fluids*, 1, 548 (1958).
36. G. E. Smith and E. E. Hirschfelder, Jr., *J. Chem. Phys.* 13, 1623 (1950).
37. W. F. Giauque and E. E. Hirschfelder, Jr., *J. Chem. Phys.* 16, 2364 (1947).
38. T. Gerasch and J. Ferguson, *Collection Czechoslov. Chem. Commun.* 22, 953 (1954).
39. T. Gerasch and J. Ferguson, *Collection Czechoslov. Chem. Commun.* 20, 149 (1955).
40. E. E. Hirschfelder, Jr. and M. J. Weiss, "Atomic Collision Processes," Ed. by R. E. O. Nelson, pp. 1073-79, North Holland Publishing Co., Amsterdam (1964).
41. E. G. Dyer, F. O. Brickwood, and G. E. Hargis, *Phys. Rev.* 122, 164 (1962).
42. E. Gerasch and M. J. Polanyi, *Z. Physik. Chem.* 253, 643 (1952).
43. G. Herzberg, "Spectra of Diatomic Molecules," pp. 350-38, Van Nostrand, New York (1959).
44. E. Spring and A. Hirschman, *J. Chem. Phys.* 1, 343 (1953).
45. J. Farkas and E. Wigner, *Trans. Farad. Soc.* 52, 708 (1956).
46. J. O. Hirschfelder, E. Spring, and E. Topley, *J. Chem. Phys.* 2, 183 (1954).
47. J. Wheeler, E. Topley, and E. Spring, *J. Chem. Phys.* 2, 176 (1954).
48. J. Sigalman, *J. Chem. Phys.* 12, 675 (1949).
49. E. L. Hirschman, *J. Phys. Collid.* 21, 635 (1953).
50. E. L. Hirschman and W. F. Jones, *Nature* 155, 790 (1952).
51. W. F. Jones, *J. Chem. Phys.* 31, 2043 (1959).

52. H. Weiss, *Elastic Collisions of Rare Gas Ions and Ionized Atoms with Neutral Molecules* (Ph.D. Dissertation, University of Florida, April, 1963); H. H. Kuehlitz, Jr. and H. J. Weiss, *Trans. Intern. Conf. Physics of Electronic and Atomic Collisions*, London (1963) 1079 (1965).
53. H. H. Kuehlitz, Jr., H. J. Randolph, and J. E. Rathi, *Rev. Sci. Instr.*, **33**, 645 (1962).
54. W. E. Craver and A. H. Marcus, *J. Chem. Phys.*, **32**, 126 (1960).
55. W. E. Craver, *J. Chem. Phys.*, **31**, 895 (1959).
56. S. Kachany, *Elastic Collisions of Hydrocarbon Cation Ions in Gases and Liquids* (Ph.D. Thesis, University of Florida, December, 1964).
57. A. Weiss and L. Reihl, *Phys. Rev.*, **125**, 375 (1962).
58. B. Berkling, B. Reihl, E. Kruuse, E. Schulz, Ch. Schlier, and P. Tschak, *Z. Physik*, **168**, 406 (1963).
59. T. F. Sibulac, B. H. Rosen, and H. Kruuse, *J. Chem. Phys.*, **32**, 2045 (1960).
60. E. H. Eftuna, T. Sasaki and J. G. Larrabee, *J. Chem. Phys.*, **33**, 902 (1961).
61. E. H. Eftuna, T. Sasaki, and J. G. Larrabee, *J. Chem. Phys.*, **33**, 912 (1961).
62. W. E. Craver and J. E. Rathi, *J. Chem. Phys.*, **25**, 1270 (1957).

BIOGRAPHICAL SKETCH

James Herbert Pechen was born on December 5, 1896, in Jackson, Mississippi. He attended elementary school in Columbia, Mississippi and graduated from Columbia High School in June, 1917. In June, 1921, he received the Bachelor of Science degree from Mississippi College, with a major in chemistry. In September, 1921, he entered the Graduate School of the University of Florida, where he held an assistantship in the Department of Chemistry and worked toward the degree of Doctor of Philosophy. Also, while at the University of Florida, he held National Science Foundation and Petroleum Research Foundation graduate fellowships.

James Herbert Pechen is a member of the Lambda Chi Alpha social fraternity.

This dissertation was prepared under the direction of the chairman of the candidate's supervisory committee and has been approved by all members of that committee. It was submitted to the Board of the College of Arts and Sciences and to the Graduate Council, and was approved as partial fulfillment of the requirements for the degree of Doctor of Philosophy.

November 18, 1965

E. R. Smith
Dean, College of Arts and Sciences

Dean, Graduate School

Supervisory Committee:

E. C. Manning Jr.
Chairman
C. E. Reid
J. A. G. G. G.
J. A. G. G. G.
J. A. G. G. G.